

A NOVEL APPROACH TO PLANETARY ROVER GUIDANCE, NAVIGATION AND CONTROL BASED ON THE ESTIMATION OF THE REMAINING USEFUL LIFE

Original

A NOVEL APPROACH TO PLANETARY ROVER GUIDANCE, NAVIGATION AND CONTROL BASED ON THE ESTIMATION OF THE REMAINING USEFUL LIFE / Rimani, Jasmine; Lizy-Destrez, Stéphanie; Viola, Nicole. - ELETTRONICO. - (2020). ((Intervento presentato al convegno International Astronautical Congress -2020.

Availability:

This version is available at: 11583/2848015 since: 2020-10-09T15:37:39Z

Publisher:

IAC

Published

DOI:

Terms of use:

openAccess

This article is made available under terms and conditions as specified in the corresponding bibliographic description in the repository

Publisher copyright

(Article begins on next page)

IAC-20,D1,4A,10,x59710

A NOVEL APPROACH TO PLANETARY ROVER GUIDANCE, NAVIGATION AND CONTROL BASED ON THE ESTIMATION OF THE REMAINING USEFUL LIFE

Jasmine Rimani^{1, *}, Stéphanie Lizy-Destrez², and Nicole Viola³

¹ Department of Mechanical and Aerospace Engineering, Politecnico di Torino, Torino, Italy, Email: jasmine.rimani@polito.it,
Department of Aerospace Vehicles Designs and Control, ISAE-SUPAERO, Toulouse, France,

Email:jasmine.rimani@isae-supero.fr

² Department of Aerospace Vehicles Designs and Control, ISAE-SUPAERO, Toulouse, France, Email:
stephanie.lizy-destrez@isae-supero.fr

³ Department of Mechanical and Aerospace Engineering, Politecnico di Torino, Torino, Italy, Email:nicole.viola@polito.it

* Corresponding author

Email: jasmine.rimani@polito.it

Abstract

This decade will be remembered as the one in which humankind will be back on the lunar soil. Research centers, industries, and universities are showing a great interest in future missions toward the Moon. The establishment of a permanent human outpost and the exploitation of in-situ resources seems to be the main drivers of this new exploration era. However, on a more engineering wise point of view, the Moon can be the perfect testbed for autonomous operations and deep space exploration enabling technologies. In this framework, the mission operations of a lunar rover are deeply linked to the performances of the guidance, navigation and control subsystem (GNC). Likewise, these performances are tied to the state of health of the system, measured by parameters like the battery level. The study presented in this paper analyzes an adaptive and autonomous GNC system for a lunar rover. The GNC relies on the failure identification, isolation and recovery subsystem (FDIR) to estimate the available resources to autonomously plan a path. More in detail, the guidance node will choose the best path to visit a series of waypoints with different rewards based on their scientific return. This new approach answer the needs of deep space exploration systems where the communication links are scarce and there is a need for autonomy and adaptability to unforeseen events. There is a shift of paradigm where the Earth's mission control leaves some decision-making tasks to the exploration system to primarily preserve the well-being of the mission. Thanks to the small-time delay with Earth, the Moon can be the perfect site to test and tune these new approaches. Overall, the GNC will be composed of a navigation node, a guidance node, a resource estimation node, and a control node. The first node will simultaneously map and localize the rover in the lunar environment. The resource estimation node will continuously evaluate the remaining useful life (RUL) of the system. Moreover, it will continuously monitor the health parameters of the system. Eventually, the proposed algorithm will autonomously generate the best plan to maximize mission return while preserving the system's health and avoiding obstacles. The algorithm may decide to skip some low reward waypoints in order to preserve resources to reach more interesting sites. The key points of the proposed algorithm are the adaptability of unforeseen events and the onboard decision autonomy to optimize the path of the rover.

Keywords: Operations, Planetary Rovers, Planning Algorithms, Lava Tubes, Routing Problems .

Acronyms

DC Direct Current

DOF Degrees of Freedom

ECSS European Committee for Space Standardization

EKF Extended Kalman Filter

FMECA Failure mode, effects, and criticality analysis

FTA Failure Tree Analysis

GNC Guidance Navigation and Control

HDDL hierarchical domain definition language

IMU Inertial measurement Unit

ISAE-SUPAERO Institut Supérieur de l'Aéronautique
et de l'Espace

LRO Lunar Reconnaissance Orbiter

PID Proportional Integrative Derivarive

PoliTO Politecnico di Torino

ROS Robot Operating System

RUL Remaning Useful Life

SaCLaB Space Advanced Concepts Laboratory

1. Introduction

This decade has seen a rise in the interest on the Moon human colonization of both space agencies and industries [1], [2]. The Earth's natural satellite can become the gate toward the exploration of Mars and beyond. It can be exploited as a testing facility to advance disruptive technologies fundamentals for both robotic and human space exploration. The foreseen exciting aim is the creation of a permanent human colony on the Moon. Among the sites of interest as future human settlement, the lunar lava tubes have been selected as possible targets [3], [4]. Various studies have shown that that the temperature and radiation environment inside this volcanic architecture may be more human-friendly than any other place on the equatorial region of the Moon [5], [6]. The focus of the scientific community lays mainly in threes lava tubes, Mare Ingenii, Mare Tranquillitatis, Marius Hills fig. 1. They have been detected and studied thank to satellite missions such as Kaguya/Selene, LRO and Clementine[7]–[10]. However, from the satellite images is difficult to understand the effective morphology of those underground tunnels, their dimensions and their geological characterization. Therefore, precursor robotic missions are envisioned for mapping the lava tubes, assess their safety for humans and study their geological characteristics [3], [4]. Due to the challenging communication set-up during the lava tube exploration [3], [4], the foreseen exploration systems should be able to operate autonomously between the different communication windows. They should be able to map their surroundings, understand and choose their targets, and decide the best path to follow. At the same time, they should be able to monitor the "health" of their critical subsystems and act accordingly to their resources while planning the trajectory. They should be able to respect a E3 level of autonomy of the ECSS space segment operability standard. Therefore, one of the most critical aspects of the missions related to the lava tubes is deeply linked to operations. More in general, the operational domain is associated with many challenges with both robotic and human space exploration. As space exploration missions grow in complexity, there is a need to balance the mission return, the autonomy level and the workload of the control centre operators. Different space agencies, companies, and universities are engaged in the definition of a broad spectrum of technological maturation studies toward autonomous operations and navigation [11]–[14]. In this context, the SaCLaB team at ISAE-SUPAERO and PoliT0 are collaborative working on new algorithms to enhance the autonomous operations of space robotic systems. The reference mission is the exploration of the lava tubes. While the systems under study are a rover and a

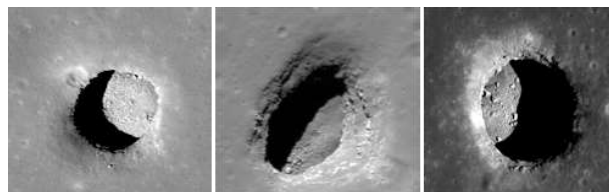


Figure 1: Lava tubes (Marius Hills, left; Mare Ingenii, center; Mare Tranquillitatis, right). Image from SELENE and LRO missions [3].

drones' swarm, dedicate to mapping and characterize the lava tubes. With the word "drone", it is identified a hopping/flying system equipped with a thruster that can perform small flight when required (for example during the descent on the lava tube from the skylight). The focus is the operational layer: the information related to the overall health of the systems is considered as an essential statistic to design more autonomous systems. This paper focuses on the rover related operations.

The rover should map the lava tubes from the surface of the Moon and release the drones in the proximity of the tubes. The study started with the analysis of its "traverse mode operations". In this paper, all the operations that engage the mobility system of the rover to move on the lunar surface are labelled as "traverse mode's operations". During the nominal mode of the "traverse operations" the rover may switch between two main operative modes: (i) "Local Reactive" when there are many obstacles in the map, (ii) "Light Local Guidance" when the map has fewer obstacles fig.2. The software used to study and carry on the mission analysis and to define the operations is Vitech Genesys 7.0 [15].

During the traverse, the rover consumes the energy stored in the batteries. In case of faults like a stuck motor or a parasitic current, the total available energy will draw faster from the rover. Therefore, it becomes interesting studying an algorithm that can help the rover reconfiguring its path based on the available RUL. The rover should be able to choose the shortest path that connects different sites of scientific interest. Each site of interest has a return in terms of scientific operations that the rover can perform. From the available estimated RUL, the robotic system should be able to choose the best set of sites of interest that it can cover. Similar studies have been carried on by [16], [17] on a testbed linking RUL and operations. However, the emphasis was placed on the timely detecting and recognizing a failure or a fault in the subsystems of the testing rover. Contrary, in this study, the focus is on the path planner algorithms that receive the RUL as an input to optimize the rover path. This paper aims to analyze what is usually framed as a "routing problem" applied to a rover [18], [19]. Hence, the algorithm presented in this paper target path planning and task planning. It puts together the

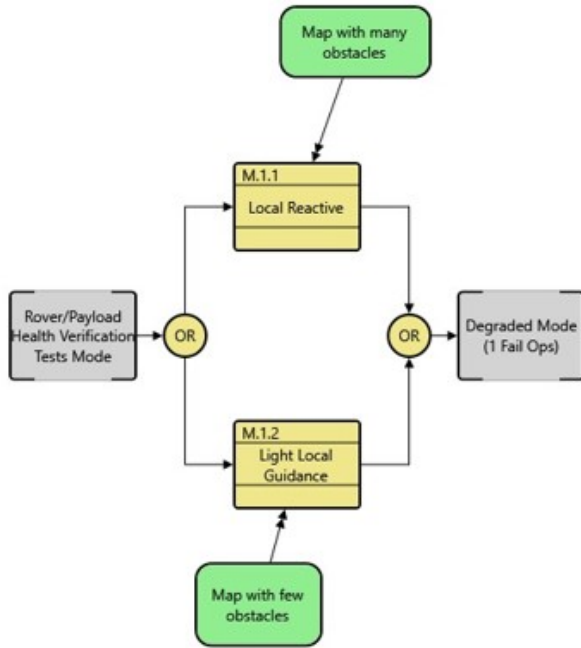


Figure 2: Nominal traverse mode for the lunar rover (Vitech Genesys 7.0 [15]).

high operational layer and the guidance layer in order to optimize the traverse operations. At a high level, a simulation framework similar to the "travel salesman problem" [20] is run. The algorithm is, then, coupled with an A* algorithm [21] as the global planner and a dynamic window [21] as a local planner. To create a challenging grid to run the global path planner, a code to lay a plausible distribution of rocks on the Moon of various dimensions and sizes is run before the actual simulation [22]. At the same time, to make the simulation more realistic, a model for batteries consumption is implemented as well as the state equations for the rover, the rover's motor and sensors [23]. In this paper, a solution to this problem is presented. The main objective is to create a planning algorithm that focuses on optimizing the operations of the lunar rover. The remaining of the paper is organized as follow: (i) 2 is introducing the framework of the study; (iii) 3 explains the mathematical and logical framework of the work as well as its result; (iv) 4 wraps-up the paper, the main outputs as well as the expected developments.

2. Case Study

The exploration mission toward the lava tubes requires a high level of autonomy: a continuous and robust communication link cannot be established underneath the lunar surface. The system that will explore the lava tubes should autonomously decide the best path to follow as well, and the most interesting targets to reach during the timeframe of one battery discharge. Following this logical flow, the

main objective of this paper is to create a task planning algorithm that can reconfigure the path of the system under study based on the available resources, e.g. the overall battery level. The robotic system that has used during the testing of the algorithms is a small skid-steered rover with an average battery autonomy of five hours. The testbed in the ISAE-SUPAERO's laboratories has been simulated both in ROS-Gazebo and with a six DOF model in Python. This model has been directly validated against the testing platform following the guidelines in [24]. It is mostly used to assess the feasibility of the studied algorithms during the first development steps. The foreseen reference mission consists of touching a series of waypoints with different scientific rewards while avoiding obstacles. During the conceptualisation of the task planning algorithm, the rover python model is used. The implemented python code keeps into account the propulsive force from the motor and the terrain friction [25]. If the Earth analogue mission is simulated, then the aerodynamic drag is considered as a force that act on the rover. Its contribution is small, however it is relevant on a small testing platform with a limited linear velocity. The 6 DOF equations are explicated from eq. 2 to eq.4.

$$\dot{\mathbf{v}} = \frac{1}{m}\mathbf{F} - \omega x \mathbf{v} \quad (1)$$

$$\dot{\omega} = \mathbf{I}^{-1}(\mathbf{M} - \omega x \mathbf{I} \omega) \quad (2)$$

$$\mathbf{F} = \mathbf{F}_p - \mathbf{F}_a - \mathbf{F}_f \quad (3)$$

$$\mathbf{M} = \mathbf{M}_p - \mathbf{M}_f \quad (4)$$

Where:

- x indicates the external product between two vectors;
- \mathbf{v} is the rover velocity;
- $\dot{\mathbf{v}}$ is the rover linear acceleration;
- ω is the rover angular velocity;
- $\dot{\omega}$ is the rover angular velocity;
- m is the rover mass;
- \mathbf{I} is the rover inertia matrix;
- \mathbf{F}_p is the force generated by the rover motors;
- \mathbf{F}_a is the aerodynamic force that act on the rover (used only for the Earth analogue simulations);
- \mathbf{F}_f is the friction force generated by the wheels' interactions with the terrain.
- \mathbf{M}_p is the moment generated by the rover motors
- \mathbf{M}_f is the friction moment generated by the wheels' interactions with the terrain.

Beyond the dynamics of the rover, the simulator takes into account a model for the wheels' DC motors in terms of current drawn, rotational velocity and motor temperature [16], [17]. The battery is simulated following the guidelines in [23]. The sensors and relative noisy readings are implemented from [16], [17], [25], [26]. The

testbed is equipped with encoders, IMU and stereo camera. The same sensors are simulated in Gazebo and reconstructed in the simulation code. During the test, in ISAE-SUPAERO an optitrack is used to estimate the rover absolute position, velocity and response to the commands. ROS gives the framework for the navigation node, using a pre-existent map and an EKF [27] for localization. The simulated map is derived from [28] elevation model, and it is explored with the build-in ROS mapping algorithms. The terrain in the lunar equatorial zone is enriched with a "likely to be" rock distribution following the guidelines from [22]. In fact, the satellite maps are not coarse enough to capture the real distribution of rocks. The same problem is experienced with Earth satellite maps. Therefore an algorithm is run before the simulation to lay a rock bad with rocks of different sizes. The rover can traverse some of the obstacles while others are too difficult to surpass. Usually, for a four skid-steered rover the maximum traversable obstacle's height is equal to half of his wheel diameter. That information is taken into account by the global path planner during its computation to estimate the best path. The control of the rover trajectory is executed with a PID controll that considers the distance from the target and the difference in "heading" between the rover trajectory and the target position.

$$v_l = v_{des} - [K_p(\psi_{des} - \psi) + K_i \int (\psi_{des} - \psi) dt + K_d(r_{des} - r)] \quad (5)$$

$$v_r = v_{des} + [K_p(\psi_{des} - \psi) + K_i \int (\psi_{des} - \psi) dt + K_d(r_{des} - r)] \quad (6)$$

Where:

- v_l is the linear velocity provided by the motors on the left side or the rover;
- v_r is the linear velocity provided by the motors on the right side or the rover;
- v_{des} is the desired velocities for the rover;
- K_p, K_i, K_d are the PID gains;
- ψ_{des}, r_{des} are the desired heading and rover angular velocity.
- ψ, r are the real heading and rover angular velocity.

The maximum reachable velocities for the motors are limited by the maximum voltage provided through the controller. In the case of the testing platform the maximum allowed linear velocity is around 0.5 m/s, while the rotational velocity is 3%.

The focus of the paper is on the guidance layer and its interaction with the task planner. The guidance associate

to the rover is divided into a global planner to estimate the best path to follow when the global map is known and a local path planner. The global path planner gives the information on a probable path length to the task planner. Two global path planners have been implemented, the A* and the D* [21]. However, the results presented in this paper are relative to the A* algorithm. The local path planner is dedicated to the refined of the trajectory to make it smooth for the rover to follow. Moreover, the local path planner avoids the unforeseen obstacles on the path of the rover. The algorithm uses the "dynamic window" path planner, as a local path planner for the rover [21].

3. Task Planning Algorithm

Fig. 3 gives a logical overview of the algorithm implemented for path planning. The objective of the task planner applied to the battery can be summarized as: *given a series of waypoints with different scientific rewards, can the rover find the best path to touch as many waypoints possible maximizing the overall scientific reward while keeping into account the overall available resources?* The algorithms start acquiring the list of interesting targets that the system should visit. The targets may be based on interesting objectives defined by the control centre or measurements from the rover cameras, or measurements conveyed by other robotic systems in the field that are collaborating with the rover. The distance can be estimated with different levels of fidelity: (i) if the obstacles presented on the field are known, it is possible to use an A* algorithm to estimate the best path; (ii) or, if the distribution is not known and cannot be estimated, it is possible to consider the geometric distance between the waypoints as the first guess. In all the cases, the planning algorithm is re-run at every site with the new reading on the overall consumed battery and the actual distance covered. In these measurements, the "guidance duty cycle" [29] is considered as well. With "guidance duty cycle" is indicate how much of the battery is dedicated to the movement during the rover mission. When, the site of interest is reached the testing rover will take a picture of the target of interest, while in the real planetary mission under design the rover will have to perform some measurements using its scientific payload. The guidance duty cycle can be linked to the overall RUL of the battery as well as the maximum reachable distance for the system. From the battery model, knowing the overall drawn current, it is possible to estimate the RUL, fig. 4. While knowing the current and the voltage of the battery, as well as the "guidance duty cycle", it is possible to estimate the rover velocity and the maximum coverable rover distance indicates as $d_{asymptotic}$, eq.7, fig.s 5 and 6.

$$d_{asymptotic} = \frac{E\eta}{C_{rr}mg} \quad (7)$$

Where:

Algorithm 1 Path Planner for battery related faults

```

1: Define list of waypoints
2: for Every waypoint ii in the list to be touched do
3:   Remove waypoints already touched
4:   Define "Guidance Duty Cycle"  $d_{gc}$ 
5:   Evaluate drawn current level  $i$ 
6:   Evaluate remaining RUL  $rul$ 
7:   Evaluate maximum reachable distance by the rover for a given current and "Guidance Duty Cycle"  $d_{coverable}$ 
8:   for Every other waypoint jj do
9:     Calculate the distance between the waypoints,  $edge_{dist}$ 
10:    if  $d_{coverable} < any(edge_{dist})$  then
11:      Stop Traverse Mode
12:      Evaluate the shortest path to touch jj waypoints from the ii waypoint,  $short_{path}$ 
13:      Evaluate the overall scientific reward,  $edge_{reward}$ 
14:      if  $edge_{dist} < d_{coverable}$  then
15:        if  $edge_{reward} < previous\ edge_{reward}$  then
16:          Store new best path
17:        end if
18:        if  $edge_{reward} = previous\ edge_{reward}$  then
19:          if  $edge_{dist} < previous\ edge_{dist}$  then
20:            Store new best path
21:          end if
22:        end if
23:      end if
24:    end if
25:  end for
26:  Provide new traffic plan to the path planner
27:  if No change in drawn current level then
28:    Go to to next waypoint
29:    if Last waypoint touched then
30:      Stop Traverse Mode
31:    end if
32:  end if
33: end for
    
```

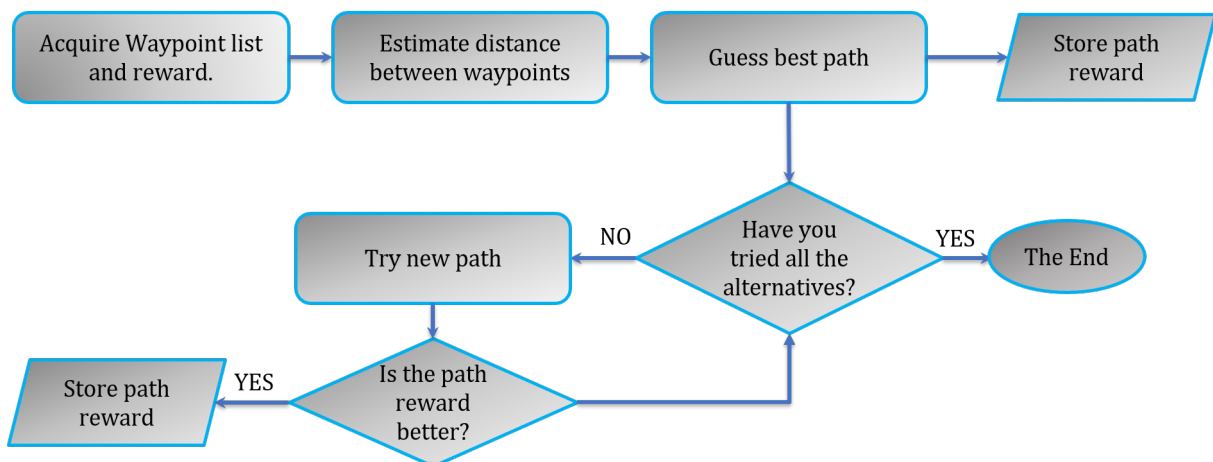


Figure 3: Flowchart explaining the logical process used for the task planning algorithm.

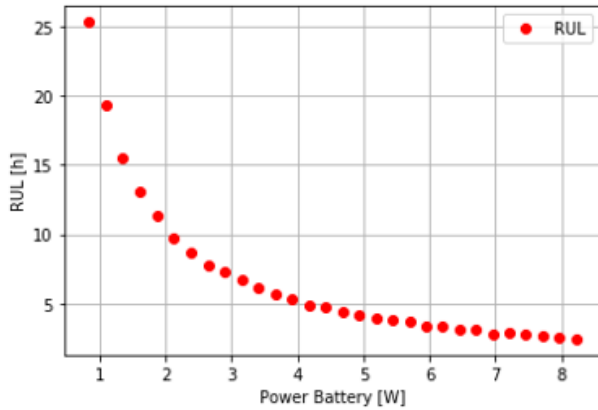


Figure 4: Battery RUL for a given consumed battery power.

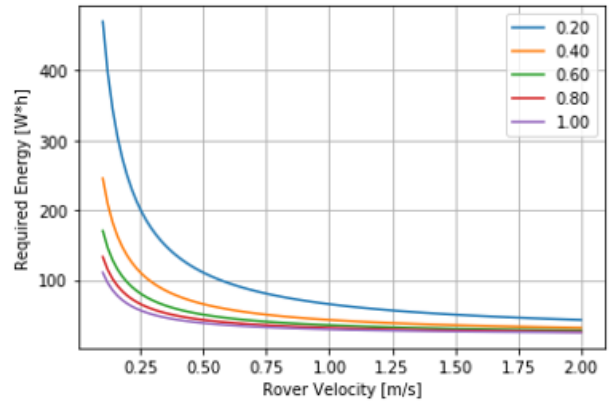


Figure 6: Required energy needed for driving with a given rover velocity, for given duty cycle (from 20% (0.2) to 100% (1.00))

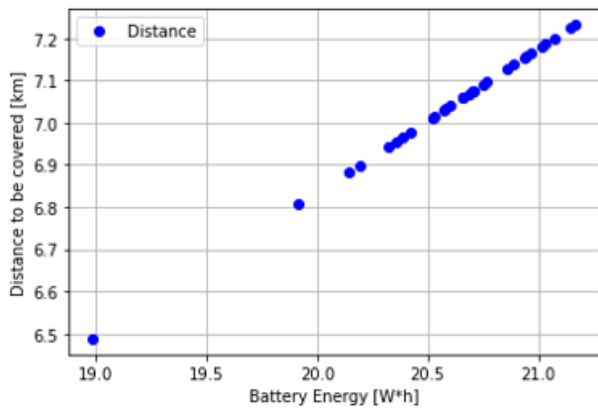


Figure 5: Maximum distance that can be covered by the rover for given battery energy and 80% guidance duty cycle.

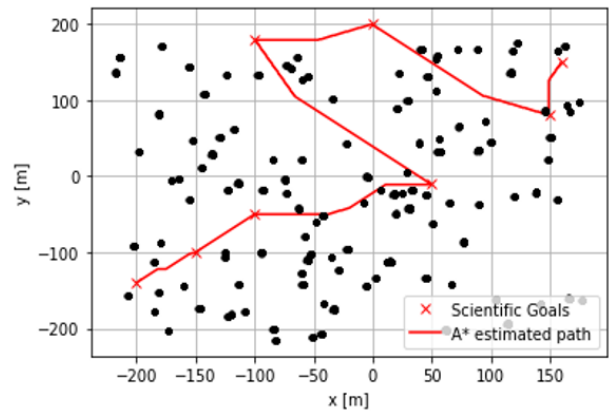


Figure 7: Shortest path to touch a series of waypoints using A* and the task planning algorithm.

- E is the battery energy;
- η is the "driving duty cycle";
- C_{rr} is the terrain resistance coefficient set at 0.15 [29];
- m is the rover mass;
- g is the gravitational acceleration.

The best path to be followed is estimated from a modify travel salesman problem [20]. One of the outputs from the implemented algorithm is the computation of the shortest path to touch a series of waypoints knowing the rock distribution, the overall free-mean space, and scientific reward for each site as shown in fig. 7. However, the algorithm is able to reconfigure the rover path based on the RUL, the chosen duty cycle, drawn current and the overall maximum allowed distance, as shown in fig. 8. Overall the task planning algorithm can provide the global path plan to be followed by the rover, given several constraints that we labelled as available resources. The path should

then be refined by the local path planner, obstacle avoidance algorithm. Moreover, the real covered distance will be updated considering the real performances of the rover moving along its trajectory such as maximum velocity and rotation rate.

4. Conclusions

The paper presents an overview of the GNC architecture that has been implemented for the system under study. The guidance layer is merged with a task planning layer to decide the best trajectory to follow based on the estimated battery level, the "guidance duty cycle", and the scientific reward of the various waypoints. The planner considers even contingency scenarios such as the one presented in this paper. Indeed, the battery may draw faster if a fault or a failure is presented in the system consuming more energy. Therefore, the current is modelled as the sum of the nominal system needs and some parasitic loads derived from faults or failures. The algorithm evaluates

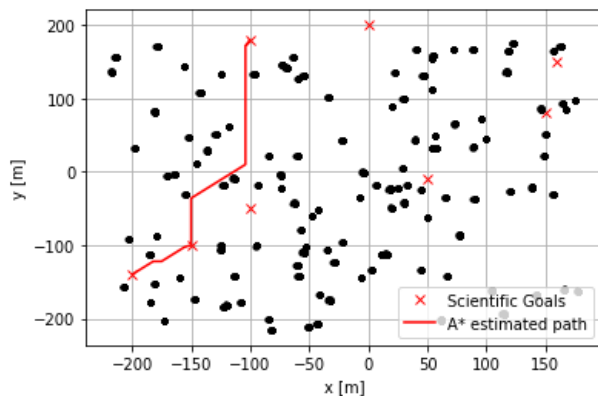


Figure 8: Reconfigure trajectory based on RUL and "guidance duty cycle".

the maximum allowed distance by the rover and estimates, which is the best path to maximize the overall scientific reward, choose the shortest path and do not consume more energy than expected during the traverse mode operations. However, beyond the faults that affect the battery, the task planner should consider faults like a stuck motor or improper sensor readings that can change the system "available" resources. These contingency situations are now under study for the traverse mode. The likelihood of a failure or a fault can be estimated from historical data available in the literature. Those data are coupled with a FTA and FMECA analysis to understand the effect of the fault, and failure, on the overall system operational layer. Therefore, the work presented in this paper will evolve toward considering the path reconfiguration in different contingency scenarios. Thus, the failure and fault analysis of the rover mobility system and GNC will be one of the expected development of the study. Nevertheless, a task planner should consider and optimize the different tasks that are foreseen for the system of interest. Hence the task planner will be extended and formalized through the use of HDDL. This extension will help to create a cluster of envisioned actions to be performed by the rover concerning different degraded scenarios.

References

- [1] ISECG, "The global exploration roadmap," *The International Space Exploration Coordination Group*, 2019.
- [2] ESA and European Commission, "The european space technology master plan," *ESTMP*, 2018.
- [3] W. Whittaker, *Technologies enabling exploration of skylights, lava tubes and caves*, 2012.
- [4] W. Whittaker, *Exploration of planetary skylights and tunnels*, 2014.
- [5] G. De Angelis and et al, *Lunar lava tube radiation safety analysis*, 2002.
- [6] T. Horvath and P. Hayne, *Thermal environments and illumination in lunar pits and lava tubes*, 2018.
- [7] S. J. Lawrence and et al., "Lro observations of morphology and surface roughness of volcanic cones and lobate lava flows in the marius hills," *Journal of Geophysical Research: Planets*, vol. 118, 2013.
- [8] T. Kaku and et al, "Detection of intact lava tubes at marius hills on the moon by selene (kaguya) lunar radar sounder," *Geophysical Research Letter*, 2017.
- [9] R. Greeley, "Lava tubes and channels in the lunar marius hills," *The Moon*, 1971.
- [10] A. G. Taylor and A. Gibbs, *Automated search for lunar lava tubes in the clementine dataset*, 1998.
- [11] Horizon-2020, *European robotic goal-oriented autonomous controller (ergo)*.
- [12] C. R. Frost, "Challenges and opportunities for autonomous systems in space," *Computer Science*, 2011.
- [13] S. Chien, R. Knight, R. Stechert A. and Sherwood, and G. Rabideau, "Integrated planning and execution for autonomous spacecraft," *IEEE Aerospace Conference*, 1999.
- [14] ESA Advanced Concepts Team, *Ai in space workshop*, 2013.
- [15] Vitech Corporation, *Genesys: Enhancing systems engineering effectiveness*, 2020.
- [16] E. Balaban, S. Narasimhan, M. Daigle, J. Celaya, et al., "A mobile robot testbed for prognostics-enabled autonomous decision making," in *Proceedings of the Annual Conference of the Prognostics and Health Management Society 2011, PHM 2011*, 2014.
- [17] E. Balaban, S. Narasimhan, M. J. Daigle, I. Roychoudhury, et al., "Development of a mobile robot test platform and methods for validation of prognostics-enabled decision making algorithms," *International Journal of Prognostics and Health Management*, vol. 4, 2013.
- [18] N. Abhishek, *Reinforcement learning with Open AI, TensorFlow and Keras Using Python*, 9. 2012, vol. 3. DOI: [10 . 1109 / MED . 2013 . 6608833](https://doi.org/10.1109/MED.2013.6608833). arXiv: [1603.02199](https://arxiv.org/abs/1603.02199).
- [19] S. Thrun, "Probabilistic robotics," *Communications of the ACM*, vol. 45, no. 3, pp. 52–57, 2002. DOI: [10.1145/504729.504754](https://doi.org/10.1145/504729.504754).
- [20] A. Blum, S. Chawla, D. R. Karger, T. Lane, et al., "Approximation algorithms for orienteering and discounted-reward TSP," *SIAM Journal on Computing*, vol. 37, no. 2, pp. 653–670, 2007. DOI: [10.1137/050645464](https://doi.org/10.1137/050645464).
- [21] A. Sakai, D. Ingram, J. Dinius, K. Chawla, et al., *Pythonrobotics: A python code collection of robotics algorithms*, 2018. arXiv: [1808 . 10703 \[cs.R0\]](https://arxiv.org/abs/1808.10703).

- [22] A. Ellery, *Planetary Rovers*. Springer-Verlag Berlin Heidelberg, 2016.
- [23] V. Sulzer, S. G. Marquis, R. Timms, M. Robinson, *et al.*, “Python battery mathematical modelling (pybamm),” *ECSarXiv. February*, vol. 7, 2020.
- [24] K. J. Worrall, “Guidance and search algorithms for mobile robots: application and analysis within the context of urban search and rescue,” 2010.
- [25] L. M. Ireland, “INVERSE SIMULATION AS A TOOL FOR FAULT DETECTION & ISOLATION IN PLANETARY ROVERS,” *GNC 2017: 10th International ESA Conference on Guidance, Navigation & Control*, DOI: [10 . 1017 / CB09781107415324 . 004](https://doi.org/10.1017/CB09781107415324.004). arXiv: [arXiv : 1011 . 1669v3](https://arxiv.org/abs/1011.1669v3).
- [26] J. Marzat, H. Piet-Lahanier, F. Damongeot, and E. Walter, “Model-based fault diagnosis for aerospace systems: A survey,” *Proceedings of the Institution of Mechanical Engineers, Part G: Journal of Aerospace Engineering*, vol. 226, no. 10, pp. 1329–1360, 2012. DOI: [10 . 1177 / 0954410011421717](https://doi.org/10.1177/0954410011421717). eprint: [https : / / doi . org / 10 . 1177 / 0954410011421717](https://doi.org/10.1177/0954410011421717).
- [27] T. Moore and D. Stouch, “A generalized extended kalman filter implementation for the robot operating system,” in *Proceedings of the 13th International Conference on Intelligent Autonomous Systems (IAS-13)*, Springer, Jul. 2014.
- [28] R. V. Wagner, E. J. Speyerer, and M. Robinson, “New Mosaicked Data Products from the Lroc Team,” in *46th Lunar and Planetary Science Conference*, 2015.
- [29] X. Xiao and W. L. Whittaker, “Energy Utilization and Energetic Estimation of Achievable Range for Wheeled Mobile Robots Operating on a Single Battery Discharge,” no. August, 2014.